Contribution from Ames Laboratory—DOE and the Department of Chemistry, Iowa State University, Ames, Iowa 50011

The Zirconium Dichloride Phase Region. Synthesis, Structure, and Photoelectron Spectral Studies of 3R-$ZrCl_2$, 6T-$Zr_{1.05}Cl_2$, and Related Phases

ALAN CISAR, JOHN D. CORBETT,* and RICHARD L. DAAKE

Received September 15, 1978

Homogenous compositions and several phases between $ZrCl_{1.5}$ ($Zr_{1.3}Cl_2$) and $ZrCl_{2.0}$ have been synthesized in sealed Ta tubing by both chemical transport reactions and isothermal equilibrations at 600–750 °C for 4–10 weeks. X-ray powder and single-crystal diffraction results indicate the breadth of the composition range is probably achieved through the formation of ordered superstructures derived from the basic three-layer slabs of the parent 3R-$ZrCl_2$ type with ordered interstitial atoms and with extensive intergrowth and twinning, the individual phases showing small if not negligible homogeneity ranges. The structure of the stoichiometric 3R-$ZrCl_{2.00(1)}$ was refined using 98 independent reflections ($2\theta \leq 60°$), space group $R3m$, a = 3.3819 (3) Å, c = 19.378 (3) Å, to R = 0.094 and R_w = 0.074. The structure consists of homoatomic layers sequenced Cl–Zr–Cl with trigonal prismatic coordination of the metal by halide (D_{3h}), isostructural with the isoelectronic 3R-MoS_2. The phase could not be intercalated. A previously reported powder pattern of $ZrCl_2$ is found to be that of monoclinic ZrO_2. A structure of 6T-$Zr_{1.047(5)}Cl_2$ (a = 3.3791 (4) Å, c = 38.713 (7) Å, space group $P\bar{3}m1$) was approximated from a crystal in which it was a minor component coherently intergrown with 3R-$ZrCl_2$ (obverse and reverse) through refinement of 266 l-odd reflections (R = 0.256). The structure consists of three subcells of the $2H_b$-MoS_2 type together with a metal atom in an interslab octahedral hole with a partial occupancy of 0.28 (3). Single-crystal evidence was also found for an 18-slab structure (a = 3.3820 (2) Å, c = 116.31 (2) Å), and powder data indicated another six-slab cell with a tripled a dimension. Twinning of 3R-$ZrCl_2$ only on slight reduction and the 6T-$Zr_{1.05}Cl_2$ structure appear to involve a common mechanism for substoichiometry—accommodation of extra metal atoms in octahedral interstices between slabs which share only edges (d_{Zr-Zr} = 3.77 Å) rather than faces (d_{Zr-Zr} = 3.23 Å) with filled trigonal prisms within the slabs. Photoelectron spectra are reported for most of the reduced zirconium chlorides. $ZrCl_2$ shows a narrow metal band 1.2 eV below E_F, well above this feature in the isoelectronic MoS_2, and is analogously a semiconductor ($E_g \approx 0.3$ eV). A metal valence band was not detected in $ZrCl_3$, and there is an abrupt increase in the Zr(3d) core levels at that point relative to more reduced phases.

Introduction

Recent investigations in this laboratory and elsewhere have elucidated the syntheses, structures, and properties of three reduced zirconium chlorides, ZrCl,[1,2] Zr_6Cl_{15},[3] and $ZrCl_3$,[4] but $ZrCl_2$ has until now remained poorly defined. The present work, undertaken to fill this gap, has in its course rectified some existing misconceptions and demonstrated the existence of a substantial region of substoichiometry for zirconium dichloride that exhibits considerable structural complexity.

Zirconium dichloride was first reported by Ruff and Wallstein in 1923 as a product either of the disproportionation of $ZrCl_3$ or of the aluminum reduction of $ZrCl_4$.[5] Since then some studies of the disproportionation of $ZrCl_3$ have *assumed* stoichiometric $ZrCl_{2.0}$ to be the product,[6,7] whereas others have analytically established this decomposition leads either to $ZrCl_{2.0}$ (manometric study in closed system[8]) or to a poorly crystalline $ZrCl_{1.6}$ (constant-weight residue from effusion studies[9]).

Over the same period two X-ray powder patterns were reported for $ZrCl_2$, both for material produced by the reduction of higher chlorides with zirconium. The first, from Swaroop and Flengas,[10] came from the product of Zr–$ZrCl_3$ reaction at 675 °C in a platinum-lined silica tube. A completely different pattern was obtained by Struss and Corbett[11] for $ZrCl_2$ produced by isopiestic equilibration of a $ZrCl_{1.4}$ mixture with excess $ZrCl_3$ at 650 °C in sealed tantalum tubes. The latter pattern was also obtained by Troyanov and Tsirel'nikov[12] for the product of controlled disproportionation of $ZrCl_3$, and they further reported the dichloride was isostructural with the isoelectronic 3R-MoS_2. However the last conclusion was based on data obtained from a nonsingle crystal, and they did not fully refine the structure (R = 0.28) or offer any explanation for the difference between the ideal composition and the analytical composition of the material from which the crystal was taken ($ZrCl_{1.87}$) other than unspecified crystal defects.

The present paper confirms that the 3R-MoS_2 structure occurs with stoichiometric $ZrCl_{2.0}$ according to refined single-crystal data. Three other polytypes of $Zr_{1+x}Cl_2$ have also been observed within a broad stoichiometry range which extends to about $ZrCl_{1.5}$, and the structure of one of these, 6T-$Zr_{1.05}Cl_2$, is reported. X-ray photoelectron spectra (XPS) of a variety of reduced zirconium chlorides are also considered. A cluster form of the dichloride, isostructural with Zr_6I_{12},[3] is not discussed in detail.

Experimental Section

Synthesis. As in other recent investigations[1-4] all reactions were carried out in tantalum tubes which had been sealed by arc welding under ≤0.5 atm of He. These in turn were jacketed in evacuated and sealed fused-silica tubes to protect them from oxidation. Starting materials for all reactions were ZrCl and $ZrCl_4$; earlier work[2,4] has shown that ZrCl can easily be produced in bulk and is a far more facile reductant for tetrachloride than is the metal. All weighings and manipulation of the compounds were carried out in a drybox under nitrogen containing 6–20 ppm of water vapor.

Microcrystalline dichloride powders were generally prepared by isothermal reaction of weighed quantities of ZrCl and $ZrCl_4$ which were mixed thoroughly and heated in a 6- or 9-mm tantalum tube at 600–725 °C for 4–10 weeks. A slight excess of $ZrCl_4$ was included to allow for the substantial pressure of $ZrCl_4$ formed by disproportionation reactions of the form

$$ZrCl_2(s) \rightarrow ZrCl_{2-x}(s) + ZrCl_4(g)$$

As a result of this reaction, all powdered samples were slightly contaminated with traces of $ZrCl_3$ through back-reaction of the tetrachloride gas with the dichloride on cooling. Such contamination was however limited to the surface as reactions in this system are generally so slow (6–8 weeks for a typical equilibration) that only a small amount of $ZrCl_3$ forms during the short time necessary for cooling in the furnace (power off), and the bulk of the material is unaffected. This contamination was reduced by minimizing the free volume of the reaction container.

Single crystals of $Zr_{1+x}Cl_2$, $0 \leq x < 0.1$, were produced by vapor phase transport via the small autogenous pressure of some reduced chloride, presumably $ZrCl_3$, in the presence of a larger pressure of $ZrCl_4$ and He. In a typical reaction 2.50 g of a ZrCl–$ZrCl_4$ mixture with a net composition of about $ZrCl_{1.3}$ was loaded into a 8.7-mm i.d. Ta tube about 14 cm long, and the tube was welded shut at the lowest pressure at which an arc could be maintained, generally about $^1/_6$ atm of He. This container was sealed in an evacuated Vycor jacket,

0020-1669/79/1318-0836$01.00/0 © 1979 American Chemical Society

and thermocouples were attached to the glass jacket about 5–7 mm inward from the actual ends of the metal container, this spacing being allowed to compensate approximately for a reduction in gradient inside the tube through the heat conduction by the tantalum. The double container with attached thermocouples was placed in an Inconel pipe at least 6 cm longer than the Vycor jacket to ensure a more even gradient. The desired gradient was achieved either by pulling the Inconel pipe out of the furnace slightly or through use of a multiple zone furnace with separate controls for each zone. Periods of 3–8 weeks were allowed for the reaction after the gradient was established.

Prior to transport the reactants were initially heated isothermally to 350 °C to affect the reduction of the bulk of the tetrachloride and then were gradually brought up to the desired temperature and gradient, care being taken to ensure that the temperature at the cool end never exceeded the desired temperature. The gradients used were 750–650, 700–650, 750–700, 850–700, and 700–750 °C, with the temperature of the starting material listed first in each case. In all cases the cooler end of the tube was elevated to promote convection within. Although the tubes used were of significantly smaller diameter than described as optimal for convection, the pressures were significantly above the 3 atm considered minimal for convective flow[13] (5–10 atm estimated with the starting material at 750 °C). Convection was believed to contribute as the rate of transport was about twice as great as at 700 °C.

Transport occurred from high to low temperature, the dichloride crystals growing in the coolest 3–5 cm of the tube. These were silvery with a metallic luster and occurred either as platelets with trigonal or hexagonal morphology, as blades with at least a 10 or 20 to 1 ratio of width to thickness, or as very thin fernlike fronds clearly exhibiting a dendritic growth pattern but still with 60 and 120° angles. Some good quality crystals could also be found intermixed with the untransported material; however crystals large enough to discern individually were usually not encountered after isothermal equilibrations even for long periods. Large crystals are stable in air for weeks, with eventual decomposition proceeding from the edges.

Transported products were obtained with compositions in the range $ZrCl_{1.75}$–$ZrCl_{2.0}$, with the exact composition dependent on temperature, gradient, and starting composition. For example, $ZrCl_{2.0}$ is obtained at 650 °C from $ZrCl_{1.75}$ at 750 °C, the relatively large gradient providing a large P_{ZrCl_4} at the cool end. A $ZrCl_{1.6}$ composition under the same conditions yields transported $ZrCl_{1.75(5)}$ (microprobe analysis) at 650 °C, while a comparable composition was obtained from $ZrCl_{1.35}$ with a large gradient (750 → 600 °C). Isopiestic, isothermal equilibrations[11] of $ZrCl_2$ or $ZrCl_3$ compositions with excess ZrCl yield a lower composition limit of $ZrCl_{1.52}$ after 4–5 weeks at 600 °C and $ZrCl_{1.6}$ at 700 °C; equilibrium is not obtained at lower temperatures. The upper limit (excess $ZrCl_3$) is $ZrCl_{2.0}$ at 750 °C; a value of $ZrCl_{1.9}$ at 650 °C may not pertain to equilibrium. The 2.0 limit can also be obtained by restricted isothermal disproportionation of known amounts of $ZrCl_3$ within tantalum tubing of known volume followed by quenching and analysis of the solid residue together with the amount of condensed $ZrCl_4$, the latter also giving good approximation to dissociation pressures. Pressures in the $ZrCl_3$–$ZrCl_2$ binary are about 5.9 atm at 500 °C and 26.8 atm at 600 °C. (Zr_6Cl_{15} must be kinetically inaccessible under these conditions as it was not encountered.) The foregoing pressures are in good agreement with an extrapolation of results reported earlier.[14] A $ZrCl_4$ pressure of 9.7 atm was in equilibrium at 600 °C with the analytical composition $ZrCl_{2.02}$ which was single phase to X-rays. Equilibration reactions in the $ZrCl_2$–$ZrCl_{1.5}$ region are markedly slower such that equilibrium cannot be obtained with $Zr_{1+x}Cl_2$–$ZrCl_3$ mixtures much below 650 °C in several weeks. The $ZrCl_{1.5}$–ZrCl dissociation pressure is about 1 atm (of $ZrCl_4$) at 700 °C.

Powder diffraction data are superficially very similar and exhibit only small shifts in lattice parameters over the entire region $ZrCl_{1.5\text{–}2.0}$, which might be taken as suggestive of a broad nonstoichiometry region. Careful examination however reveals additional lines which cannot be indexed on a primitive cell of the dimensions of $ZrCl_2$. Bands also appear between lines with indices (based on the primitive cell) of the form $h0l$ and $0h,l+1$. These features are consistent with a series of ordered superstructures, with extensive twinning and intergrowth as well being revealed by single-crystal studies.

Photoelectron Spectroscopy. Data were obtained with both X-ray (XPS) and ultraviolet (UVPS) sources using an AEI Model ES200B instrument coupled to a Nicolet 1180 minicomputer for data averaging and curve smoothing. Spectra were accumulated in either 128 channels or 256 channels for from 10 to 500 scans. Smoothing involved a nine-point fit centered on each point of of the spectrum. Data were obtained using either Al Kα (1486.6 eV) X-ray or He I (21.21 eV) ultraviolet excitation. XPS for materials without an apparent Fermi edge were referenced to silver metal on the back of the sample holder.

Samples were prepared by pressing the powdered material onto a strip of indium and attaching this to the sample holder. Most reaction containers were first opened in the helium atmosphere of a drybox which was directly connected to the sample port of the instrument and contained H_2O and O_2 at less than 1 ppm each. As a result O 1s emission was virtually absent in the XPS of samples studied. All spectra were obtained from unetched samples since argon ions were found to decompose $ZrCl_2$ to ZrCl instead of cleaning the surface.

Powder Patterns. All powder patterns were obtained using an evacuable Model XDC-700 Guinier camera (IRDAB, Stockholm) equipped with a quartz, bent-crystal monochromator adjusted to produce a Cu $K\alpha_1$ (λ 1.540 56 Å) incident beam. This unit produces a dispersion of 1° in 2θ for each 1.75 mm of film and when coupled with a measurement reproducibility of 0.01–0.02 mm for line positions yields a precision of ±0.005–0.010° in 2θ. Line positions were referenced to Si powder mixed with the sample (NBS Standard Reference Material 640, a = 5.430 88 Å). A precision scale was printed on the film before the pattern was taken using an IRDAB XDC scaling device in order to automatically compensate for nonlinear film shrinkage as well as for variations in film length arising from temperature changes during reading. Line sharpness was enhanced by only developing the front side of the film. As before[4] the powder samples for Guinier examination were mounted in the drybox on a strip of cellophane tape previously attached to a washer of proper size to fit into the camera, and the sample was covered with a disk of tape previously cut with a cork borer.

Lattice parameters were calculated from indexed patterns using a local lattice-refinement program which has provision for assigning poorly measured (weak or broad) lines a lesser weight in the refinement.[14] Calculated powder patterns were produced by the Clark, Smith, and Johnson program[15] modified to match local conventions and machine configuration and to add the appropriate Lorentz–polarization factor for the Guinier–Hägg geometry.

Single-Crystal Studies. For single-crystal studies the Ta tube was opened in a drybox specially designed for crystal mounting and described elsewhere.[1] Individual crystals with well-developed faces and maximum dimensions in the range of 0.2–0.3 mm were selected and mounted in 0.2- or 0.3-mm diameter Lindemann glass capillaries. These were sealed inside the drybox with a hot wire and again outside the drybox with a gas torch, and the ends were capped with Apiezon W wax. All crystals mounted were examined with oscillation photographs taken with a standard Weissenberg camera and Ni-filtered Cu Kα radiation as problems with crystal defects and distortions were significant. For example, the parent rhombohedral structure of 3R-$ZrCl_2$ was frequently observed to be twinned with both obverse (standard) and reverse settings present in the diffraction pattern. The conversion amounts to a 60° rotation about c between two choices of the a and b axes or, alternatively, to an interchange of a and b and inversion of c.[16] This change is accompanied by a conversion of the nonextinction condition (hexagonal settings) from $-h+k+l=3n$ (obverse) to $h-k+l=3n$, thus creating a set of unique reflections for each setting save for overlap with $h=k$. The twinning is easily recognized in the Weissenberg photograph as the possible observation of every third reflection along the festoons becomes two out of three. Many crystals were so thin in the c dimension that they bent to follow the capillary wall during mounting. Such a crystal gives good sharp spots on oscillation normal to c but produced streaks parallel to the direction of translation in a Weissenberg photograph[17] (or in an oscillation photograph taken with the film translating). This arises when a given plane of the crystal comes into diffracting position as a continuous function of rotation.

The data for structure solution and refinement were collected using an automated four-circle diffractometer designed and built in the Ames Laboratory; this and the indexing scheme have been described in detail elsewhere.[18,19] The radiation used was Mo Kα monochromatized with pyrolytic graphite (λ 0.709 54 Å) at a takeoff angle of 4.5°. During data collection the intensities of four or five different standard reflections were monitored every 75 reflections to check for instrument and crystal stability. No evidence of decay was observed.

For 3R-$ZrCl_2$ the initial orientation and extinctions indicated a C-centered monoclinic cell, and 570 reflections were examined to 2θ

< 60° for a crystal of about 0.2 × 0.2 × 0.03 mm in dimensions. All 447 of the allowed reflections in a full hemisphere were observed [$I > 3\sigma(I)$]. However the early results on the structure solution (all atoms on special positions in space group *Cm*) together with the fact that the monoclinic cell data were related by $a = 3^{1/2}b$ led to reexamination of the assignment and the conclusion that the correct space group was *R*3*m* (No. 160). (The situation is analogous to that found with ZrCl.[1]) All reflections had been examined for the rhombohedral cell, and averaging these data for $\bar{3}$ Laue symmetry yielded 98 unique reflections. A least-squares fit to the 2θ values of 20 reflections ($40° < 2\theta < 50°$), each of which was tuned to both Friedel-related peaks to eliminate instrument and centering errors, yielded trigonal lattice parameters $a = 3.3819$ (3) Å, $c = 19.378$ (3) Å, and $V = 191.94$ (4) Å^3 and a reduced axial ratio ($c/3a$) of 1.9100 (equivalent to a primitive rhombohedral cell with $a = 6.748$ (1) Å and $\alpha = 29.025$ (3)°). These results are in good agreement with those obtained earlier by indexing powder patterns on the basis of a hexagonal cell.

For 6T-$Zr_{1+x}Cl_2$, 1944 reflections with $2\theta < 60°$ in the *HKL* and $H\bar{K}L$ octants and part of the $H\bar{K}\bar{L}$ octant were examined for a crystal of similar dimensions as above. A total of 1452 of these were observed (based on $I > 3\sigma(I)$) and these reduced to 577 unique reflections on averaging for $\bar{3}$ symmetry. Because this crystal was really a coherent intergrowth of separate 6T and 3R polytypes (a problem which will be treated in detail below), the reflections tuned for lattice constant determination were sorted into two groups: one allowed for only 6T-$Zr_{1+x}Cl_2$ and the other for reflections primarily resulting from the 3R-$ZrCl_2$ component ($\pm(-h + k) + l = 3n$). The lattice parameters so obtained were $a = 3.3791$ (4) Å and $c = 38.713$ (7) Å ($V = 382.82$ (11) Å^3) for the 6T-$Zr_{1+x}Cl_2$ component and $a = 3.3793$ (2) Å and $c = 19.374$ (1) Å ($V = 191.60$ (2) Å^3) for the 3R-$ZrCl_2$ component. The difference between *c* for the 6T and 2*c* for the 3R components, 0.034 (7) Å, is probably significant but not great enough to allow the resolution of nominally superimposed reflections.

Structure Refinement of 3R-$ZrCl_2$. The initial *C*-centered space group choices were limited to *Cm* and *C*2 by cell volume plus a statistical indication of accentricity. Both require the origin be fixed, and so a single metal atom at 0, 0, 0 was used to phase an electron density map. Of the resultant choices for chlorine atoms, only that utilizing twofold positions in *Cm* refined. On recognition of the rhombohedral equivalency of the solution, where all atoms are on special positions (0, 0, *z*),[16] the zirconium atom was again fixed at (0, 0, 0) in accordance with the convention used for the isostructural MCh_2 compounds.[20] Refinement of the converted chlorine atom positions together with isotropic temperature factors for three atoms resulted in an unweighted residual $R = \sum||F_o| - |F_c||/\sum|F_o| = 0.10$.

Because of the known substoichiometry of at least some zirconium dichloride products, an electron density map was carefully examined at this point for any evidence of electron density at the interslab location between halide layers where the fractional extra atoms are found in sulfides[20] such as 3R-$Nb_{1+x}S_2$,[21] but none was found. Insertion of a fractional atom on this site produced a large increase in *R* on refinement, and variation of the occupancy of the other three atoms alone produced no significant change in *R* or in the unit occupancies. These circumstances were taken as conclusive evidence that the crystal examined had a stoichiometry of $ZrCl_{2.00(1)}$.

Conversion to anisotropic temperature factors allowed refinement to $R = 0.082$ ($R_w = [\sum w(|F_o| - |F_c|)^2/\sum w|F_o|^2]^{1/2} = 0.116$, $w = \sigma(F)^{-2}$), and reweighting of the data set to reduce a large standard deviation for an observation of unit weight led to final values of $R = 0.094$ and $R_w = 0.074$. No absorption correction was carried out as the linear absorption coefficient (μ) for this compound is only 58.6 cm^{-1},[16] and the shapes of the refined thermal ellipsoids did not suggest the need for such a correction.

Structure Determination for 6T-$Zr_{1+x}Cl_2$. The crystal utilized for this study consisted of both twinned and intergrown components. Pairs of spots from obverse and reverse 3R-$ZrCl_2$ were the dominant feature in the Weissenberg photo, but a coherent six-slab component was also present which generated an additional, weaker set of spots in the center of and between the 3R pairs. The latter also made a small contribution to the dominant 3R reflections which could not be resolved because of the close relationship between the lattice constants (vide supra).

A Patterson map calculated with all data had a peak at (0, 0, $^1/_2$) which was >90% as great as at the origin. At first thought, this could arise from a superstructure consisting of two units of the 3R structure in each cell of the 6T. This possibility failed to refine. The map also clearly shows the presence of all of the peaks expected for both settings of the 3R structure, in agreement with the Weissenberg observations that the crystal was an intergrowth of 3R-$ZrCl_2$ and 6T-$Zr_{1+x}Cl_2$. As noted above, the lattice constants could also be resolved for the two components as well. The hypothesized intergrowth was confirmed by discerning two separate structures.

First, the data subset containing only the reflections allowed for a three-slab cell in the obverse rhombohedral orientation refined to an *R* of 0.121 ($R_w = 0.174$), using the atom positions and isotropic thermal parameters previously obtained for 3R-$ZrCl_2$, with all converged atom parameters within 1σ of the values obtained previously.

A structure was deduced for the six-slab component using only the 266 reflections with odd values of *l*. Two atoms were assigned tentatively by assuming that the largest one-slab separation vector observed in the Patterson map calculated with all of the data represented a Zr–Zr vector for the six-slab component. Phasing with these two atoms revealed the location of either one more metal for a centric structure or four more for an acentric structure. Four atoms were included, assuming nothing about the symmetry, and 12 chlorine atoms located. Refinement of these atoms for both the centric and acentric possibilities proceeded in parallel until the refinement for the acentric case showed coupling between temperature factors for inversion-related atoms which was taken to indicate that the centric choice was correct.

At this point the trial structure contained a slab stacking ABABAB, equivalent to three unit cells of 2H-MoS_2,[20] which alone did not explain the observed six-slab cell. Examination of an electron density map indicated the presence of a fractional zirconium atom in a plausible site, the octahedral hole between slabs centered at (0, 0, 0). With an estimated occupancy of 0.5, the refinement proceeded to an *R* of 0.261 ($R_w = 0.400$). The occupancy was then estimated at 0.33 (5) from an integration of its peak in an electron density map relative to that of a chlorine atom. Following refinement of all other atoms and reweighting, we fixed the temperature factor of the partial atom at that of the other metal atoms, and its occupancy refined to 0.28 (3) ($R = 0.256$, $R_w = 0.298$) corresponding to a composition of $Zr_{1.047(5)}Cl_2$. There were no problems with convergence.

Although this structure (henceforth called 6T) is based on a very high-symmetry subcell (2H-MoS_2, space group $P6_3/mmc$, No. 194), its actual symmetry is relatively low, corresponding to only that of space group $P\bar{3}m1$ (No. 164). Although the structure cannot be considered fully refined, the result appears plausible as well as satisfactory given the limitations imposed on the data. First among these limitations was the use of a partial data set (*l* odd) obtained from a minor component of an intergrown crystal. The minority circumstance was very apparent in the raw data since intensities of reflections with $l \neq 2n$ were systematically one-third or less than those with $l = 2n$. The lack of *l*-even data was naturally clearly revealed in the electron density synthesis by the appearance of a negative map of each half of the known structure at $z + {}^1/_2$. In spite of the rough contours, no more atoms were indicated; none of 12 small but conceivable new atom locations in this map refined to a meaningful occupancy (>3σ and >0.06 Zr).

The 00*l* data appear the least satisfactory, with F_o generally too large, such that R_w drops by 30% when these are excluded. This situation could arise indirectly from either anisotropic secondary extinction or absorption. The first could be significant when *h* and *k* are relatively large for a crystal which is relatively perfect in the *a* and *b* directions, while the second would arise from low absorption (F_o high) in the very thin direction of the crystal (*c*). The second is considered much more likely since the major portion of the crystal was not under study, a circumstance which would in effect raise the absorption coefficient by perhaps a factor of four or five. However, an absorption correction was not considered profitable. The quality of the data do not allow a significant refinement with anisotropic parameters, although the modest elongation of metal thermal ellipsoids apparent in the *c* direction probably reflected both absorption and the usual dominance of stacking defects normal to this direction. The crystal exhibited moderate streaking along the festoons, indicative of further unresolved disorder. Other crystals of the "phase" gave much more streaking.

A further limitation on the solution could have been imposed by the superposition of nonequivalent reflections. If the crystal had been single, this would not occur, but the 6T component might have been twinned to a degree comparable to that signaled for the 3R component by the presence of both obverse and reverse reflections. In space group

Table I. Atomic Parameters for 3R-$ZrCl_2$

atom	z[a]	B_{11}[b]	B_{33}
Zr	0.0	0.41 (7)	1.02 (9)
Cl(1)	0.2449 (3)	0.72 (14)	1.1 (2)
Cl(2)	0.4220 (3)	0.75 (14)	1.2 (2)

[a] All atoms are on 3*a* positions in $R3m$ with $x = y = 0$. [b] Anisotropic temperature factors are in units of A^2 and of the form $\exp[-1/4(B_{11}h^2a^{*2} + B_{22}k^2b^{*2} + B_{33}l^2c^{*2} + 2B_{12}hka^*b^* + 2B_{13}hla^*c^* + 2B_{23}klb^*c^*)]$. $B_{22} = 2B_{12} = B_{11}$ and $B_{13} = B_{23} = 0$.

Table II. Interatomic Distances (Å) and Angles (deg) for 3R-$ZrCl_2$

Distances		
Zr–Zr	3.3819 (3)	closest Zr, same slab
Zr–Zr	6.7479 (3)	nearest Zr, next slab
Zr–Cl(1)	2.598 (4)	nearest neighbor coordination
Zr–Cl(2)	2.601 (4)	
Zr–Cl(1)	4.746 (6)	nearest Cl, next slab
Cl(1)–Cl(1)	3.3819 (3)	translation within layer
Cl(2)–Cl(2)	3.3819 (3)	
Cl(1)–Cl(2)	3.431 (7)	same slab (trigonal prism)
Cl(1)–Cl(2)	3.603 (6)	nonbonding, interslab

Angles			
Cl(1)–Zr–Cl(2)	82.6 (1)	Cl(2)–Zr–Cl(2)	81.1 (1)
Cl(1)–Zr–Cl(1)	81.2 (1)	Cl(1)–Zr–Cl(2)	135.88 (4)

$P\bar{3}m1$ two equivalent possibilities for the selection of the *a* and *b* axes also differ by a rotation of 60° about the *c* axis. Depending on which choice is made, the same plane will have different indices (121 and $3\bar{1}1$ for example), but these indices are not equivalent by symmetry and do not interconvert. As a result, a crystal so twinned yields intensities for each *hkl* reflection which are the averages of the two nonequivalent contributions. The structure 6T-$Zr_{1.05}Cl_2$ could be solved only because the $2H_b$ subcell has higher symmetry for which these reflections *are* equivalent.

Results

The stoichiometry range possible with the $ZrCl_2$-type phases varies only slightly with temperature over the accessible range. From 600 to greater than 700 °C the lower limit is near $Zr_{1.33}Cl_2$ ($ZrCl_{1.5}$) while the oxidized limit appears to increase slightly from about $Zr_{1.05}Cl_2$ ($ZrCl_{1.9}$) at 650 °C to $ZrCl_2$ at 700 °C and above, although the single-crystal data indicate that there is a two-phase region somewhere in that range just below 700 °C. Equilibrium is achieved only slowly (weeks) at the lower temperatures quoted for at each limit, so that mixtures of phases ($ZrCl_2$ plus ZrCl or $ZrCl_3$) are obtained even when the overall composition lies in the range $1.6 < Cl:Zr < 2.0$. Clearly numerous other slab-type dichlorides must exist in this system below $Zr_{1.05}Cl_2$ which have not yet been identified (isolated as single crystals).

Structure of 3R-$ZrCl_2$. Table I contains the positional and thermal parameters for 3R-$ZrCl_2$ and Table II the interatomic distances and angles. The observed and calculated structure factors appear in the supplementary material. Figure 1(a) depicts the (110) section of the structure.

Although the only point symmetry required for the trigonal prism surrounding the zirconium in $ZrCl_2$ is C_{3v}, the observed symmetry is D_{3h}. The two independent Zr–Cl distances differ by only 0.003 (6) Å, and the angles between the central metal atom and each pair of end atoms are identical.

Careful examination of the pattern reported for $ZrCl_2$ prepared by metal reduction of $ZrCl_3$ in a platinum-lined silica tube at 675 °C[10] now reveals that the product was actually Baddeleyite, the low-temperature (monoclinic) form of ZrO_2.[22] The black color reported for the product must have arisen from a small amount of either reduced chloride or finely divided metal undetected by X-ray diffraction. The sharpness reported for the pattern indicates that the oxide was produced at high temperature rather than during subsequent handling at room temperature.

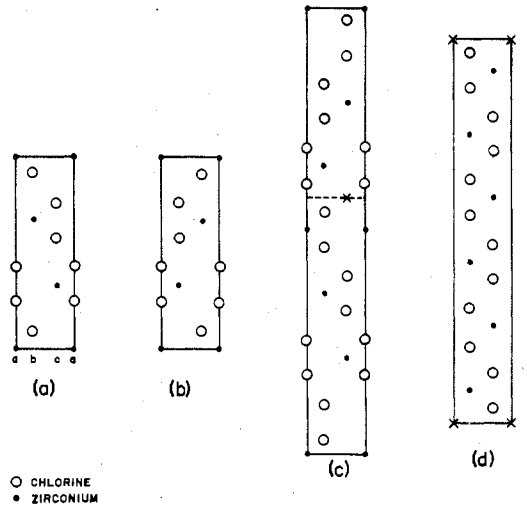

Figure 1. Schematic (110) sections of various slab-type dichlorides (large open circles = chlorine; small solid circles = zirconium): (a) 3R-$ZrCl_2$, obverse orientation; (b) same, reverse; (c) possible twin mechanism with obverse (lower) and reverse (upper) orientations and an octahedral hole (×) on the boundary (see text); (d) structure proposed for 6T-$Zr_{1+x}Cl_2$, × marking octahedral intersticies for extra metal atom ($x = 0.05$ for 28% observed occupancy).

Table III. Atomic Positions for 6T-$Zr_{1.05}Cl_2$

atom	x	y	z (obsd)	z (ideal)	B, A^2
Zr(1)	1/3	2/3	0.0815 (1)	0.0833	0.4 (2)
Zr(2)	2/3	1/3	0.2489 (2)	0.2500	0.4 (2)
Zr(3)	1/3	2/3	0.4182 (2)	0.4167	0.5 (2)
Zr(4)[a]	0.0	0.0	0.0		0.5
Cl(1)	2/3	1/3	0.0352 (7)	0.0390	2.6 (4)
Cl(2)	2/3	1/3	0.1227 (7)	0.1277	2.7 (4)
Cl(3)	1/3	2/3	0.1986 (11)	0.2057	4.2 (6)
Cl(4)	1/3	2/3	0.2923 (6)	0.2943	1.9 (4)
Cl(5)	2/3	1/3	0.3756 (5)	0.3724	1.2 (3)
Cl(6)	2/3	1/3	0.4590 (12)	0.4610	4.6 (7)

[a] Occupancy refined to 0.28 (3) with *B* fixed at 0.5, corresponding to Zr:Cl = 1.047 (5):2

On the other hand, the present results confirm in detail the structure proposed for $ZrCl_2$ by Troyanov and Tsirel'nikov[12] on the basis of incomplete structural study ($R = 0.28$). The present investigation yielded both positions and interatomic distances to about one more significant figure which otherwise agree with theirs. (The reported[12] intraslab Cl–Cl separation of 3.06 Å must be a misprint of 3.60 Å.)

Powder data for a phase near $ZrBr_2$ in composition can be indexed on a hexagonal cell with $a = 3.5257$ (2) Å and $c = 13.726$ (2) Å (26 reflections).[23] The dimensions and the intensities of the reflections observed agree semiquantitatively with those expected for a two-slab structure in space group $P6_3/mmc$, the most common examples of which are $2H_a$-NbS_2 and $2H_b$-MoS_2. Unfortunately the $ZrBr_2$ was part of a mixture with ZrBr which interfered with intensity measurements and made further conclusions regarding the correct structure ($2H_a$ or $2H_b$) inconclusive, but it seems clear that this compound also has trigonal prismatic coordination of the metal. This result is only partially in agreement with a report which assigns $ZrBr_2$ the 3R structure based on a nine-line powder pattern (eight lines of which can be explained by the $2H_b$ structure) plus a partial examination of a single crystal;[24] however $ZrBr_2$ could well be dimorphic.

Structure of 6T-$Zr_{1.05}Cl_2$. The atomic positional parameters for 6T-$Zr_{1.05}Cl_2$ appear in Table III. The values in the column marked *z* (ideal) are based on a unit cell having three subcells of the $2H_b$ type,[20] full $P6_3/mmc$ symmetry, and the same intraslab Cl–Cl separation as observed in 3R-$ZrCl_2$. The

Table IV. X-ray Photoelectron Spectra Maxima for Zirconium Chlorides (eV)

level	Zr[a]	ZrCl	$ZrCl_{1.6}$[b]	$ZrCl_{\sim 2.0}$[c]	Zr_6Cl_{12}	$ZrCl_3$	$ZrCl_4$[d]
Zr(4d)	0.8	1.15	1.2	1.2	1.45		
Cl(3p)		6.4	6.5	6.6	6.5	6.0	5.0
Cl(3s)		17.3	17.9	17.6	17.3	17.0	*e*
$Zr(3d)_{5/2}$	178.8	179.4	180.1	180.2	179.9	182.2	182.8
$Zr(3d)_{3/2}$	181.2	181.8	182.5	182.7	182.6	184.4	185.2
$Cl(2p)_{3/2}$		199.6	200.0	200.0	199.1 sh 199.6	199.7	198.5
$Cl(2p)_{1/2}$		201.2	201.6	201.5	200.7 sh 201.1	201.2	200.1

[a] From ref 25. [b] $Zr_{1.25}Cl_2$. [c] 3R structure. Data given were obtained from two specimens and standardized by reference to the Zr(3d) and Cl(2p) core levels. [d] From ref 2. [e] Not reported.

actual symmetry is $P\bar{3}m1$, with all of the atoms except Zr(4) on the 2*d* special position which restricts (*x*, *y*) to (1/3, 2/3) or (2/3, 1/3). Atom Zr(4) is on the 1*a* position (0, 0, 0). The observed and calculated structure factors for the partial set of reflections used to determine the structure of 6T-$Zr_{1.05}Cl_2$ appear in the supplementary material.

A (110) section of the structure proposed for 6T-$Zr_{1.05}Cl_2$ appears in Figure 1(d). Save for small chlorine displacements (Table III), the structure is nearly equivalent to three cells of the $2H_b$-MoS_2 type with one extra metal atom in an octahedral hole every six slabs. Because of the degree of refinement, little can be gained through comparison of distances within the structure. The average Zr–Cl closest separation, 2.57 (2) Å, and the intraslab and interslab Cl–Cl distances, 3.33 (3) and 3.59 (4) Å, are insignificantly different from those in 3R-$ZrCl_2$.

18T-$Zr_{1+x}Cl_2$ and Other Variations. Among the many crystals examined, several gave compelling evidence for the existence of more cell types than the two refined above and their twin–intergrowth combinations. Weissenberg photographs taken of several crystals revealed three additional reflections were present along the festoons between pairs of reflections which had the indices *h*0*l* and *h*,0,*l* + 1 based on a 3R-sized cell. The extra spots were spaced so that the entire set of five reflections had relative separations of 2:1:1:2, indicating that these were the center three from the series of five which would be expected in that interval for a unit cell with 18 slabs in the repeating sequence.

This evidence allowed several previously unindexable lines in some powder patterns to be understood and lattice parameters to be obtained for this variation (which will be designated 18T in the absence of any symmetry information). The latter are a = 3.3820 (2) Å, c = 116.312 (15) Å (V = 1152.1 (2) Å^3), and $c/18a$ = 1.9106. The length of c is only slightly greater (0.044 (23) Å) than 6 times that in 3R-$ZrCl_2$, but no further conclusions can be drawn without knowledge of the composition of the phase. It is not possible to resolve individual reflections for such a cell with an automated diffractometer even with copper radiation, and although data could be obtained with film techniques, it was not considered worth the large investment of time this would entail, especially for an intergrown crystal.

Four lines frequently appeared in powder patterns of $Zr_{1+x}Cl_2$ compositions which could not be fully explained by any of the varieties of $ZrCl_2$ described above. All of these irregular ones can be indexed (as 100, 103, 333, and 338) on a unit cell with a equal to 3 times that found in all of the foregoing and six slabs to the repeating sequence in c. While this may be sufficient data to define the lattice size of this supercell (a = 10.146 Å and $c \simeq$ 38.77 Å), there are so many possible arrangements for a cell of this size given the demonstrated trends to polymorphism and supercell formation that speculation on its structure is pointless. This structure is definitely distinct from the 6T structure; the four reflections in question were searched for on the 6T data crystal with the diffractometer but were not found.

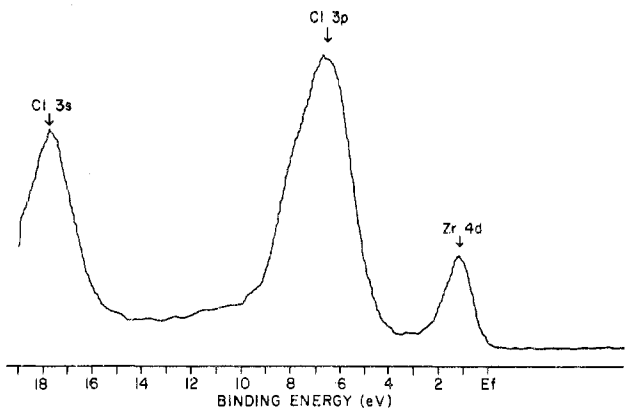

Figure 2. Valence region of the XPS of slab-type dichloride with an actual composition of $ZrCl_{1.6}$ (monochromatized, smoothed, 440 scans, ±0.2 eV). The spectrum of 3R-$ZrCl_2$ shows negligible differences.

Finally, a distinctly different type of zirconium dichloride occurs with the cluster compound Zr_6Cl_{12}, which has been deduced to be isostructural with Zr_6I_{12}[3] from powder patterns.

Photoelectron Spectra. Figure 2 shows an X-ray photoelectron spectrum (XPS) for $ZrCl_2$-type phases while Table IV lists the XPS peak maxima of most of the known zirconium chlorides. Spectra were also obtained for the $ZrCl_2$-type phases with a He I source; although the Zr(4d) band was then generally slightly smaller and sharper relative to Cl(3p) and the $Cl(3p_{3/2})$–$Cl(3p_{1/2})$ transitions were partially resolved, the results served mainly to confirm the XPS results. The slab-type dichloride spectra given in the table are not labeled as to polytype because of the difficulty in obtaining powder specimens which are assuredly only one polytype, but it is unlikely that the difference between polytypes would be detectable by XPS, the spectra being almost entirely dependent on the bonding within the slab. The same valence spectrum was obtained for $ZrCl_{1.6}$ and a specimen of pure 3R-$ZrCl_2$. The values for ZrCl found here are within 0.1 eV of those obtained previously on another instrument, and so it can be assumed that the values for $ZrCl_4$ would agree as well.

The Zr(3d) (core) levels, Table IV, show the expected monotonic increase in binding energy with oxidation state with an overall shift of 4 eV between Zr^0 and $ZrCl_4$. The change is not linear however, with somewhat over half of the increase coming between $ZrCl_2$ and $ZrCl_3$, the same place where the Zr(4d) (valence) band disappears (to XPS). The results of Table IV are thus in contradistinction to the behavior observed with the metal $L\alpha_{1,2}$ edges in X-ray emission[26] both in the presence of a break at $ZrCl_2$ and in the very similar metal core level observed with the limited delocalization in the Zr_6Cl_{12} cluster. Trends in core level energies per se rather than in differences in energies of M and L levels, both of which are known to vary in a substantially parallel manner in XPS, would seem to be more readily interpretable.

In elemental zirconium ($4d^4$) the valence band is centered at 0.8 eV below the Fermi edge[25] with a sizable density of ionization states at that level, as expected. In ZrCl($4d^3$) the 4d band maximum has shifted to 1.1$_5$ eV, and the density of states at E_F is lower,[2] again as expected. (Band calculations confirm that the valence band is mostly Zr(4d) with little involvement of chlorine orbitals, and a similar behavior would be expected in $ZrCl_2$.[27]) The shift in position for Zr(4d) levels on going from ZrCl to the slab-type dichloride ($4d^2$) is negligible in view of a measurement uncertainty of about 0.3 eV. But, compared with Cl(3p), the metal 4d band in $ZrCl_2$ is narrower than in ZrCl as well as being significantly smaller, consistent with a threefold change in the ratio of 4d electrons to chloride. As shown in Figure 2, the narrowing of the metal valence band without shift causes the apparent density of occupied states at the Fermi level to drop to zero, consistent with the semiconduction found for slab-type $ZrCl_2$ (below). The metal–metal separation in 3R-$ZrCl_2$, 3.38 Å, is relatively large compared with 3.09 Å in ZrCl (intersheet) or 3.18 Å in α-zirconium, but the results of Figure 2 suggest a narrow band rather than localized states is present. The absence of a shift of valence or core spectra on reduction from $ZrCl_{2.0}$ to $ZrCl_{1.6}$ may reflect either the dominance of the normal slab spectrum over that of minority interstitials or the oxidation of surface layers on cooling.

Although the ratio of Cl(3p) to Zr(4d) electrons drops another factor of three between $ZrCl_2$ and $ZrCl_3$, a comparable metal valence band should probably still be visible with $ZrCl_3$, other factors being equal, and its absence is somewhat of a surprise. This compound is a relatively poor conductor in spite of contrary expectations for the idealized structure;[4,28] a substantial number of zirconium displacements to ideally vacant octahedral intersticies as well as reduced orbital size for zirconium(III) could be responsible for both observations. The concomitant and sudden increase in Zr(3d) binding energy on oxidation from $ZrCl_2$ to $ZrCl_3$ presumably reflects an appreciable increase in electron localization and a decrease in screening which took place in the more reduced chlorides through small but appreciable s and p contributions to the band.

Finally, the Cl(3p) (valence) levels, Table IV, show no discernible trend. There is however a small shift in Cl(2p) to *higher* binding with reduction ($\leq$1.5 eV), with most of the change coming between $ZrCl_3$ and $ZrCl_4$. The shift is contrary to simple ionicity arguments and implies covalent bonding and participation of chlorine in formation of a nominal 4d metal band on reduction, an effect which is quite prominent with the sulfides.[25,29] (A low charge on chlorine would of course be expected to be a necessity for the formation of the layered compounds ZrCl and $ZrCl_2$.)

Well-formed blades or plates of $ZrCl_2$ up to 2 mm long as formed in long-term transport reactions have a high reflectance and metallic luster. Notwithstanding, two-probe measurements yield low conductivities ($\geq 10^{-5}$ ohm^{-1} cm^{-1} at 20 °C, $E_g \approx 0.3$ eV) in agreement with the inferences from XPS data.

Although intercalation is an important part of the chemistry of the slab-type dichalcides,[30] all attempts to intercalate $ZrCl_2$ were unsuccessful. Direct reaction with liquid NH_3 (3 h at −20 °C followed by 17 h at −80 °C) produced only a small amount of NH_4Cl. Potassium and sodium in ammonia (16 h at −50 °C) produced only NH_4Cl and KCl as identifiable new products. Pyridine (24 h at 20 °C) produced what was evidently $ZrCl_3 \cdot 2py$.[31]

Discussion

The 3R structure found for $ZrCl_2$ makes it isostructural with a number of dichalcides, e.g., NbS_2, TaS_2, and MoS_2 plus the selenides of the same elements.[20] The trigonal-prismatic coordination of metal by nonmetal found in 3R-$ZrCl_2$ is rare among halides while being relatively common among chalcides. Only for ThI_2 has any other refined crystal structure shown trigonal-prismatic coordination of a metal by halide, and in this structure half of the cations have the more common octahedral coordination.[32] Although similarities between sulfides and chlorides are definitely the exception rather than the rule,[33] in this case $ZrCl_2$ also conforms to the criterion recognized for semiconducting dichalcides with trigonal-prismatic coordination as in MoS_2, namely, a d^2 configuration. In this symmetry, d orbitals will be split into a_1', e′, and e″, and in a localized description[34] the first is fully occupied in MoS_2 and half filled in metallic NbS_2. The same conclusions are reached in band-structure calculations by APW methods.[35] Covalency is doubtlessly of greater importance in this structure for chalcides.[29]

Although the photoelectron emission spectra of 3R-MoS_2 and 3R-NbS_2 are not available for comparison with $ZrCl_2$, those of 2H-MoS_2 and 2H-$NbSe_2$ are.[36,37] In any case, bonding within the slabs is expected to be so dominant that a difference in packing is unlikely to have a measurable effect. The spectrum of $NbSe_2$ supports the observed metallic behavior. Both measurements and calculations classify MoS_2 as a semiconductor, and this is seen particularly clearly in the UVPS results where the highest occupied band, principally Mo(4d), is centered 2.5 eV below the Fermi level with at least a 1 eV gap between the top of the band and E_F.[37] The spectra also show an overlap in binding (ionization) energy between the metal valence and the S(3p) bands, consistent with a substantial orbital mixing in the dichalcide. The isoelectronic but less covalent $ZrCl_2$ appears to fit in very nicely. The greater separation and lower mixing between metal and halide states would mean the highest filled band is more nearly pure Zr(4d) in character, as in ZrCl.[27] Zirconium should have both a higher energy and a greater extension of the 4d orbitals than molybdenum as a result of its lower nuclear and formal charge, although this size difference is probably compensated for by the greater covalency in the sulfide. The narrowness of the 4d valence band, Figure 2, suggests that the metal–metal overlap in $ZrCl_2$ is less than that in MoS_2. Relative metal distances do not seem particularly useful in this comparison; that within the sheets in $ZrCl_2$ is only 6% greater than in the metal, much closer than the 15% considered significant in MoS_2 where d_{Mo-Mo} = 3.16 Å.[38] The gap implied by the location of E_F, Figure 2, suggests that a narrow, filled band, $(a_1')^2$ in a localized sense, is split off from the remainder of the empty d-like states, similar to but less extensively and with less mixing with metal states than in MoS_2.

Structures of the Substoichiometric Dichloride Phases. In contrast to the foregoing similarities with disulfides, the $ZrCl_2$ system apparently achieves substoichiometry in a different way and degree than known among chalcides. Among the related MCh_2 compounds, those with group 5 metals [(Ta, Nb)(S, Se)$_2$] are metallic and exhibit continuous, wide substoichiometry ranges and much polytypism. In all, substoichiometry is evidently achieved by the random insertion of additional metal atoms into the octahedral holes between the slabs, generally with no loss in symmetry or enlargement of the unit cell. On the other hand the group 6 dichalcides (Mo, W)(S, Se)$_2$ isoelectronic with $ZrCl_2$ show no evidence of nonstoichiometry and only two polytypes (3R and 2H$_b$).[20]

Zirconium dichloride differs significantly from both of these by achieving a wide substoichiometry range through the formation of, as far as have been characterized, only ordered polytypes, each with a composition range which is limited and possibly negligible. This type of behavior is somewhat similar to that of $Ti_{1+x}S_2$ where all metal atoms have octahedral coordination.[39] Some plausible reasons for these differences can be deduced. If symmetry is to be maintained on reduction

of the 3R structure, there is only one site available for extra metal atoms, the octahedral hole between the slabs located at (0, 0, $^5/_6$) (and two other equivalent points; Figure 1). This arrangement is observed with 3R-$Nb_{1.06}S_2$,[21] but no evidence for the occupation of this interstitial site could be found in either the crystal of 3R-$ZrCl_2$ or the 3R component of reduced mixed single crystals. However it will be noted that occupation of this site in 3R-$ZrCl_2$ would result in a 3.23 Å Zr–Zr separation, vs. 3.38 Å within the slabs, so that this event would presumably be accompanied by some form of interaction, in a localized sense between filled a_1' (d_{z^2}) orbitals. But either a bonding or a repulsive interaction can be avoided by an alternative accommodation for the extra atoms, either at a twin boundary (at low concentrations) or in the 6T structure.

Figure 1(c) shows such a mechanism for the former. The order is depicted as rhombohedral obverse at the bottom and reverse at the top, and an extra metal atom (indicated by X) is inserted at the octahedral hole between slabs. In the slab above, the trigonal prism which normally holds the metal atom is then left vacant, and that atom is instead displaced to the adjacent trigonal prism in order to avoid the short (3.23 Å) metal–metal distance. This is equivalent to having the occupied trigonal prism share an edge rather than a face of the occupied octahedron. From this point the stacking continues as before. The shift at the occupied interstice is equivalent to a rotation of the coordinate system by 60° about *c* which converts the stacking from obverse to reverse rhombohedral orientation. This process produces (1) a minimum metal–metal distance of 3.77 Å from the octahedral atom between the slabs where the stacking slip occurs and (2) a twinned crystal. Actually a real crystal may have many such boundaries, but the observed sharpness of the diffraction spots suggests the fault occurs no more often than about every 1000 Å and perhaps much less. The substoichiometry introduced at this level is of course analytically negligible. Although the crystal of 3R-$ZrCl_2$ on which data were collected was free of detectable twinning, twinned 3R crystals are frequently observed growing in the region just hotter (more reduced) than that where the untwinned crystals are found, supporting the occurrence of this twin mechanism for absorbing small amounts of extra metal or, alternatively, the *requirement* of extra metal atoms for twinning. This potential mechanism was described as "chemical twinning" by Andersson and Hyde.[40]

Eventually some concentration limit will be reached at which the extra metal atoms begin to interact with each other and develop a periodicity. As noted earlier in the Results section, several larger unit cells are observed, and of these 18T-$Zr_{1+x}Cl_2$ appears to be the best candidate for a simple interstitial ordering. This phase, found on samples just slightly reduced from $ZrCl_{2.0}$, is the largest yet reported for layered compounds based on trigonal-prismatic coordination of metal. (A 12-slab TaS_2 supercell based on 6R-TaS_2 has been reported but not further characterized.[41]) The extreme length of the *c* axis in 18T precludes convenient X-ray examination.

Further reduction yields 6T-$Zr_{1.05}Cl_2$, a phase which equals 6R-TaS_2[20] as the longest repeat cells characterized and is the first found with only trigonal-prismatic slabs. The structure is approximately equivalent to three unit cells (six slabs) of the $2H_b$-MoS_2 type with an extra metal atom in an octahedral hole every six slabs, Figure 1(d), and, analogous to the postulated twinning mechanism, in Figure 1(c), shows a second effective way to order atoms in octahedral interstices with minimal interaction of these with metal within normal slabs. The $2H_b$-MoS_2 substructure in this is unique in several respects; it is the only slab-type structure which occurs exclusively for d^2 compounds, and it is the only arrangement with exclusively trigonal-prismatic coordination of the metal where every metal has two second nearest neighbor nonmetals directly above and below the triangular ends of the prism, viz., ···B CbC BcB C···. (The situation is analogous to ZrBr vs. ZrCl;[2] ThI_2 also has this ordering but also has half the cations in octahedral coordination.) This MoS_2-type structure is also the only arrangement in which an extra metal atom in an octahedral hole between slabs shares only edges, not at least one face, of its coordination sphere with the trigonal prism about another metal atom. These features maximize nonmetal–metal and minimize metal–metal interactions between slabs and would seem to be particularly important in the structures occurring for the substoichiometric $ZrCl_2$.

Equilibration results suggest 3R, 18T, and 6T are adjacent and interrelated phases. The fact that 18T-$Zr_{1+x}Cl_2$ has only been observed in samples equilibrated at over 700 °C and cooled rapidly (relative to the multiweek periods needed to approach equilibrium) suggests that it may be only metastable below 700 °C. At this temperature 18T has an equilibrium $ZrCl_4$ partial pressure of >5 atm, and this climbs rapidly to over 30 atm at 800 °C for compositions in the neighborhood based on the degree of tube bulging. Powder pattern evidence of 18T is found only in samples just slightly reduced from $ZrCl_{2.0}$ in composition, suggesting its composition is approximately $ZrCl_{1.95\pm}$, with the upper limit presumably in equilibrium with twinned 3R-$ZrCl_2$ (t-3R).

The fact that 6T-$Zr_{1+x}Cl_2$ was *always* found intergrown with t-3R is a strong indication that some variation, probably 18T, forms at high temperature and on cooling disproportionates by ionic diffusion and slab slippage to t-3R at the reduced limit and 6T at the oxidized limit, presumably near $Zr_{1.05}Cl_2$. If this decomposition temperature is high enough to ensure good ionic mobility, which it seems to be, numerous regions of the crystal will separate into intergrown microcrystals with all of their axes in register. That this diffusion mechanism is not perfect, and that all of the atoms do not always end up in their equilibrium positions, is clear from the streaks observed along the festoons in all of the Weissenberg photographs of the crystals of this type. These streaks, which with some crystals rivaled the 6T reflections in intensity, connected reflection pairs of the type *h*0*l* allowed for either the obverse or reverse rhombohedral setting and *h*,0,*l* + 1 allowed for the other. In powder specimens, bands often connect these reflection pairs.

Since the 6T variation is a superstructure of the $2H_b$, not the 3R, stacking scheme, the 6T phase should be very apparent if a significant amount were present in a powder specimen. Notwithstanding, the only evidence found for the existence of this compound is a minority component of single crystals intergrown with 3R-$ZrCl_2$. This behavior is not understood. Exactly where the six-slab structure with $a' = 3a_{3R}$ fits is difficult to say. It is observed in many, if not most, substoichiometric powder specimens.

Acknowledgment. The authors are indebted to Professor R. A. Jacobson for the use of the four-circle diffractometer and for advice on several crystallographic problems, to J. W. Anderegg for obtaining the XPS and UVPS spectra, to Dr. T. Y. Hsiang for the conductivity measurements, and to Professor B. N. Harmon for useful discussions. The instrument on which the spectra were measured was made available by a grant from the National Science Foundation to the Department of Chemistry, Iowa State University. This work was supported by the U.S. Department of Energy, Office of Basic Energy Sciences, Materials Sciences Division.

Registry No. $ZrCl_2$, 13762-26-0; ZrCl, 14989-34-5; $ZrCl_3$, 10241-03-9.

Supplementary Material Available: Structure factor data for 6T-$Zr_{1.05}Cl_2$ and 3R-$ZrCl_2$ (2 pages). Ordering information is given on any current masthead page.

References and Notes

(1) D. G. Adolphson and J. D. Corbett, *Inorg. Chem.*, **15**, 1820 (1976).
(2) R. L. Daake and J. D. Corbett, *Inorg. Chem.*, **16**, 2029 (1977).
(3) J. D. Corbett, R. L. Daake, K. R. Poeppelmeier, and D. H. Guthrie, *J. Am. Chem. Soc.*, **100**, 652 (1978).
(4) R. L. Daake and J. D. Corbett, *Inorg. Chem.*, **17**, 1192 (1978).
(5) O. Ruff and R. Wallstein, *Z. Anorg. Allg. Chem.*, **128**, 96 (1923).
(6) A. G. Turnbull and J. A. Watts, *Aust. J. Chem.*, **16**, 947 (1963).
(7) K. Uchimura and K. Funaki, *Denki Kagaku*, **33**, 163 (1965).
(8) S. I. Troyanov and V. I. Tsirel'nikov, *Russ. J. Phys. Chem. (Engl. Transl.)*, **48**, 1174 (1974).
(9) D. B. Copley and R. A. J. Shelton, *J. Less-Common Met.*, **20**, 359 (1970).
(10) B. Swaroop and S. N. Flengas, *Can. J. Chem.*, **43**, 2115 (1965).
(11) A. W. Struss and J. D. Corbett, *Inorg. Chem.*, **9**, 1373 (1970).
(12) S. I. Troyanov and V. I. Tsirel'nikov, *Vestn. Mosk. Univ. Khim.*, **28**, 67 (1973).
(13) H. Schäfer, "Chemical Transport Reactions", Academic Press, New York, 1964, pp 11–14.
(14) F. Takusagawa, Iowa State University, personal communication, 1976.
(15) C. M. Clark, D. K. Smith, and G. G. Johnson, "A FORTRAN IV Program for Calculating X-ray Powder Diffraction Patterns—Version 5", The Pennsylvania State University, University Park, PA, 1973.
(16) "International Tables for X-ray Crystallography", Vols. 1 and 3, Kynoch Press, Birmingham, England, 1952 and 1968.
(17) G. H. Stout and L. H. Jensen, "X-ray Structure Determination", Collier-Macmillan, London, 1968, pp 83–147, 270–99.
(18) D. R. Schroeder and R. A. Jacobson, *Inorg. Chem.*, **12**, 210 (1973).
(19) R. A. Jacobson, *J. Appl. Crystallogr.*, **9**, 115 (1976).
(20) F. Hulliger, "Structural Chemistry of Layer-Type Phases", D. Reidel, Boston, MA, 1976, pp 234–42, 270–73.
(21) D. R. Powell and R. A. Jacobson, to be submitted for publication.
(22) "Powder Diffraction File 1969", American Society for Testing and Materials, Philadelphia, PA, 14–534.
(23) R. L. Daake, Ph.D. Thesis, Iowa State University, 1976.
(24) G. S. Marek, S. I. Troyanov, and V. I. Tsirel'nikov, *Vestn. Mosk. Univ. Khim.*, **32**, 64 (1977).
(25) T.-H. Nguyen and H. F. Franzen, Iowa State University, unpublished research.
(26) G. P. Kostekova, Yu. P. Kostikov, S. I. Troyanov, and D. V. Korol'kov, *Inorg. Chem.*, **17**, 2279 (1978).
(27) J. Marchiando, B. N. Harmon, and S. H. Liu, unpublished results.
(28) R. G. Clemmer, *Diss. Abstr. Int. B*, 674 (1977).
(29) H. F. Franzen, *Prog. Solid State Chem.*, **12**, 1 (1978).
(30) F. R. Gamble and T. H. Geballe in "Treatise on Solid State Chemistry", Vol. 3, N. B. Hannay, Ed., Plenum Press, New York, 1976, pp 89–203.
(31) G. W. A. Fowles and G. R. Willey, *J. Chem. Soc. A*, 1435 (1968).
(32) L. J. Guggenberger and R. A. Jacobson, *Inorg. Chem.*, **7**, 2257 (1968).
(33) J. D. Corbett, submitted for publication in *Adv. Chem. Ser.*
(34) C. Haas in "Crystal Structure and Bonding in Inorganic Chemistry", C. J. M. Rooymans and A. Rabenau, Eds., North-Holland Publishing Co., Armsterdam, 1975, pp 103–25.
(35) L. F. Matheiss, *Phys. Rev. B*, **8**, 3719 (1973).
(36) G. K. Wertheim, F. J. DiSalvo, and D. N. E. Buchanan, *Solid State Commun.*, **13**, 1225 (1973).
(37) J. C. McMenamin and W. E. Spicer, *Phys. Rev. B*, **16**, 5474 (1977).
(38) J. A. Wilson and A. D. Yoffe, *Adv. Phys.*, **18**, 236 (1969).
(39) R. J. D. Tilley in "Crystallography and Crystal Chemistry of Materials with Layered Structures", F. Levy, Ed., D. Reidel, Boston, MA, 1976, pp 159–69.
(40) S. Andersson and B. G. Hyde, *J. Solid State Chem.*, **9**, 92 (1974).
(41) A. H. Thompson, *Solid State Commun.*, **17**, 1115 (1975).

Contribution from the Department of Chemistry, State University of New York at Buffalo, Buffalo, New York 14214

Structural Studies on Polynuclear Osmium Carbonyl Hydrides. 10. Molecular Geometry and Comments on the Location of the μ_2-Hydride Ligand in $(\mu\text{-H})Os_3W(CO)_{12}(\eta^5\text{-}C_5H_5)$[1]

MELVYN ROWEN CHURCHILL* and FREDERICK J. HOLLANDER

Received August 16, 1978

The heteronuclear tetrahedral cluster derivative $(\mu\text{-H})Os_3W(CO)_{12}(\eta^5\text{-}C_5H_5)$ has been studied by means of a single-crystal X-ray structural analysis. The complex crystallizes in the noncentrosymmetric orthorhombic space group $P2_12_12_1$ [D_2^4; No. 19] with a = 9.2707 (14) Å, b = 11.8539 (23) Å, c = 19.7258 (33) Å, V = 2167.7 (6) Å^3, and ρ(calcd) = 3.544 g cm^{-3} for Z = 4 and mol wt 1156.69. Diffraction data were collected with a Syntex $P2_1$ diffractometer and the structure was refined to R_F = 5.6% and R_{wF} = 4.6% for those 1446 reflections with $|F_o| > 3\sigma(|F_o|)$ and $4.0° < 2\theta < 45.0°$ [Mo Kα radiation]. The molecule contains a tetrahedral cluster of metal atoms in which the tungsten is coordinated to an η^5-C_5H_5 ligand and two terminal carbonyl ligands and in which each osmium is associated with three terminal carbonyl ligands. There is, in addition, a bridging carbonyl ligand across the Os(1)–W(4) bond and a bridging hydride ligand across the Os(2)–Os(3) vector. Consideration of bond lengths and cis M–M–L angles reveal that the bridging hydride ligand lies in, or close to, the Os(1)–Os(2)–Os(3) plane.

Introduction

The heteronuclear metal carbonyl hydride $(\mu\text{-H})Os_3W(CO)_{12}(\eta^5\text{-}C_5H_5)$ has previously been prepared by the reaction of $Os_3(CO)_{10}(NCMe)_2$ with $HW(CO)_3(\eta^5\text{-}C_5H_5)$.[2] A single-crystal X-ray structural analysis of $(\mu\text{-H})Os_3W(CO)_{12}(\eta^5\text{-}C_5H_5)$ has been undertaken in order to determine the location of the bridging hydride ligand and the overall connectivity within this complex tetranuclear species.

Experimental Section

A. Collection of X-ray Diffraction Data. Dark red transparent crystals of $(\mu\text{-H})Os_3W(CO)_{12}(\eta^5\text{-}C_5H_5)$ were supplied to us by Professor J. R. Shapley of the University of Illinois at Urbana-Champaign. The columnar crystals generally showed a hexagonal cross section and often gave evidence of twinning parallel to the long axis of the crystal. A "house-shaped" crystal of approximate dimensions 0.18 × 0.20 × 0.25 mm was cleaved from one of the columnar crystals. Careful examination under a polarizing microscope gave no evidence of twinning. The crystal was mounted on a glass fiber and sealed into a thin-walled glass capillary tube which was fixed in an aluminum pin and mounted in a eucentric goniometer. Preliminary precession photographs indicated *mmm* (D_{2h}) Laue symmetry (i.e., suggested the orthorhombic crystal class) and confirmed the crystal quality. The crystal was transferred to a Syntex $P2_1$ automated diffractometer and oriented with the a^* axis approximately 8.5° from the spindle axis (ϕ) of the diffractometer. Crystal alignment, determination of the orientation matrix and accurate cell dimensions, and data collection were all carried out as described previously.[3] Details specific to the present analysis are listed in Table I. The systematic absences $h00$ for $h = 2n + 1$, $0k0$ for $k = 2n + 1$, and $00l$ for $l = 2n + 1$ uniquely define the noncentrosymmetric nonpolar space group $P2_12_12_1$ (D_2^4; No. 19).

All crystallographic computations were performed using our Syntex XTL system,[4] which is comprised of (i) and in-house Data General Nova 1200 computer with 24K of 16-bit word memory and with a parallel floating-point processor for 32- and 64-bit arithmetic, (ii) a Diablo moving-head disk unit with a capacity of 1.2 million 16-bit words, (iii) a Versatec electrostatic printer/plotter, and (iv) the XTL conversational crystallographic program package, as modified by our

0020-1669/79/1318-0843$01.00/0 © 1979 American Chemical Society